Journal of Physics: Conference Series **117** (2008) 012002 doi:10.1088/1742-6596/117/1/012002

Quantum study of tungsten interaction with beryllium (0001)

A Allouche[1] and Ch Linsmeier[2]

[1]Physique des Interactions Ioniques et Moléculaires, CNRS and Université de Provence, Campus Scientifique de Saint Jérôme, service 242, 13397 Marseille Cedex 20 - FRANCE

[2]Max-Planck-Institut für Plasmaphysik, EURATOM Association, Boltzmannstr. 2 85748 Garching b. München, GERMANY

E-mail: alain.allouche@univ-provence.fr

Abstract. Beryllium, tungsten and carbon are planned as wall materials for the future international tokamak (ITER). Be and W will be the dominant components and therefore the formation of binary Be-W alloys under plasma action is one of the most important issues in plasma-wall interaction processes at the first wall. The formation of alloys and their reactivity under physical sputtering and chemical erosion constitute a new challenge for solid states physics and chemical reactivity. This article proposes a theoretical study of the first stages of the formation of these alloys based on the *first principles* DFT method. The tungsten adsorption energy on the basal (0001) beryllium surface is first calculated, and then the barrier to retention into the bulk. For each calculation the electronic structure of the formed compound is analyzed through density of states (DOS) calculation. The results are discussed with respect to experimental observations during the formation of a $Be_{12}W$ alloy layer and changes in the electronic structure of Be during alloying, observed in shifts of the Be 1s core levels.

1. Introduction

A tokamak [1] is a toroidal device where a deuterium (D) – tritium (T) plasma is magnetically confined in order to reach energy and concentration high enough to induce the thermonuclear fusion of the two nuclei, thus releasing a very large amount of energy:

$$D + T \rightarrow He\ (3.5\ MeV) + n\ (14.1\ MeV)$$

Nuclear fusion of light atoms is the fundamental process in the Sun, which provides energy and light to our solar system. ITER (acronym standing for International Thermonuclear Experimental Reactor) is an international research tokamak proposal, which is intended as an experimental project of magnetic confinement for future power generation through thermonuclear fusion. According to the ITER consortium, fusion power offers the potential of "environmentally benign, widely applicable and essentially inexhaustible" electricity [2]; properties that they believe will be needed as world energy demands increase while simultaneously greenhouse gas emissions must be reduced. ITER is being built in Cadarache (France) starting in 2007.

Although the inner wall of the tokamak is isolated from the hot plasma by confinement in magnetic fields, the wall is still subjected to ion, atom and other fragment fluxes issued from a much colder plasma region named the boundary plasma. Therefore, the inner wall cladding of a tokamak is made

up of materials of specific mechanical, magnetic, thermal and electric properties: the ITER's first wall will be constituted of beryllium (690 m^2), tungsten (140 m^2) and carbon (55 m^2). The plasma particles (whose energies range from a few eV to several 100 eV) will induce chemical erosion and physical sputtering processes that will give rise to deposition of a thick beryllium film on the tungsten part and contamination of the beryllium surface by tungsten atoms originating from the boundary plasma. As a consequence the wall cladding will no longer be constituted of pure metals but rather made up of alloys of unknown composition and chemical behavior.

Experimental simulations have been proposed in recent years, notably by the R Doerner [3] and the Ch Linsmeier [4] groups. However, the fundamental processes underlying the alloy formation mechanisms can only be completely elucidated through theoretical contributions. Therefore a new field of investigation is open for the computational quantum communities, going from solid-state physics to surface physics and catalysis. The latter domain and chemical reactivity are more particularly involved because of hydrogen retention: the chemistry of these materials towards hydrogen isotopes retention is largely unknown. Hydrogen retention in the tokamak inner wall (specially the radioactive isotope T) is of utmost importance for safety reasons: if the trapped tritium mass exceeds a few hundreds grams, the machine operation must be stopped.

Therefore, the quantum theory and the first-principles Density Functional Theory (DFT) are the most reliable approach to determining the fundamental processes of the first steps of beryllium – tungsten mixed materials formation together with their reactivity towards the nuclei and radicals provided by the boundary plasma.

2. Computational section

The calculations were performed within the framework of the spin-polarized gradient-corrected density functional theory (DFT). The exchange, as well as the correlation, functionals are Perdew-Burke-Ernzerhof PBE. A plane-wave basis set was used with an energy cutoff of 32 Rydberg (435 eV); the ionic core potential was modeled using Vanderbilt ultrasoft pseudopotentials. Integration in the first Brillouin zone was performed using the 6x6x1 points Monkhorst-Pack sampling.

The stationary state structures were optimized using the Quasi-Newton Broyden-Fletcher-Goldfarb-Shanno generalized algorithm. All the atoms were included in the optimization procedure, without any geometry or symmetry constraint. All the energy calculations were carried out using the *Quantum-Espresso* package [5]. The tungsten pseudopotential is taken from the package's library and then carefully tested.

3. Results and discussion

3.1. Metallic beryllium

The electronic configuration of a beryllium atom is $1s^2 2s^2$. As a consequence, the isolated atom behaves mostly as a rare gas atom; i.e. the calculated dimer dissociation energy D_e is only 0.06 eV (CCSD(T)) or 0.16 eV (B3LYP) [6], and the inter-atomic distance is very long for a second row element, R_e = 2.49 Å. These values are consistent with experiment: D_e = 0.12 eV [7] and R_e = 2.45 Å [8].

A consequence of this particular condition is that a Be cluster, as large as it can be considered, would not converge towards the bulk limit. The DFT calculated binding energy per atom of a neutral Be_n (n=2-21) cluster converges to 2.0 eV (LDA) [9] or 2.41 eV (GGA-BPW91) [10].

In their pioneer work, Dovesi et al. [11] performed a periodic Hartree-Fock *CRYSTAL* [12] calculation. They found a -slightly too large- crystal parameter $\boldsymbol{a}$ = 2.32 Å, but their binding energy was notably underestimated: 1.87 eV (exp. 3.3 eV [13]). They ascribed the difference versus the experimental value to the electronic correlation energy, which they presumed to contribute up to 1.36 eV per atom to the crystal cohesive energy. At that time, the calculation of correlation energy was not included in the *CRYSTAL* code.

The Vanderbilt ultrasoft pseudopotential we optimized for the beryllium yields the resulting crystal parameters (close-packed hexagonal structure: ***a*** = ***b*** = 2.28 Å (experimental 2.29 Å [13]), ***c***/***a*** = 1.54 (exp: 1.57). The cohesive energy was calculated as a difference between the total energy and the energy of a free atom in a cubic cell of box length = 5 Å, its value being 3.7 eV. Therefore, PBE slightly overestimates the correlation energy, but the results are in good agreement with previous DFT results [14],[15]. The crystal cell parameter ***a*** (notably shorter than in the HF calculation mentioned above) is in reasonable agreement with experiment, although the ratio ***c***/***a*** is 1.9 % too small.

Figure 1a shows the electronic density of states near the Fermi level. The most important feature is the large participation of the 2*p* states in the valence band and even in the lowest conduction band. Compared to the clusters calculations, it is clear that the *s*-*p* hybridization is more efficient in the crystal orbitals than in the cluster ones and that the bulk cohesion is mainly insured by these orbitals. The *pseudo gap* near the Fermi level, already mentioned by Dovesi et al., is analyzed by Häussermann et al. in [16]. According to these authors, the pseudo gap is due to the large orbital hybridization that raises the *s*-*s* antibonding part of the band above the Fermi level. It is clear also from Figure 1a that the *s* state contribution at the Fermi level is zero.

The beryllium (0001) basal plane substrate is represented by a 5-layer slab (44 Be atoms) of dimension = 6.864 x 6.864 Å. The vacuum, of 10 Å, is large enough to annihilate the interaction between two successive cells in the ***c*** direction (Figure 2a).

The calculated surface relaxation is negligible, maybe because of the small size of the slab. Some other calculations concluded also that the surface is not reconstructed [17]. Other calculations using 12 layers and LDA functional found a relaxation of only 3.2 % between the upper two layers [18] while a 9-layer GGA yields 2.5 % [15]. Nevertheless, a very small charge transfer is observed from the surface to the inner layers since the total electronic charge of the surface atoms is 1.97 electron.

Figure 1 compares the bulk and (0001) DOS. The pseudo gap remains in the film as in the bulk but the valence band structure appears more complex because of the differentiation of the σ and π-type *p* orbitals. The in-plane bonds insured by p_x+p_y functions prevail upon the inter-layer bonding (p_z functions).

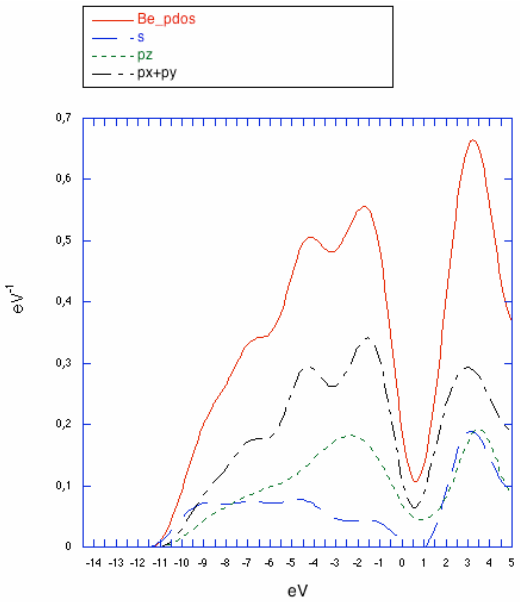

Figure 1a: Electronic Density of States (DOS) of bulk beryllium. The origin of energies is fixed at the Fermi level (also in the other figures).

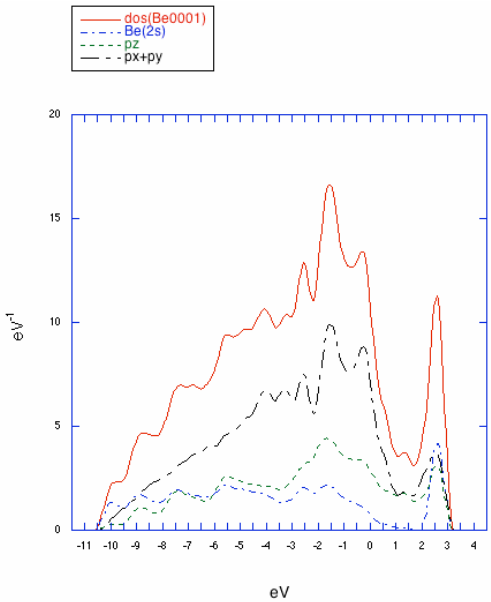

Figure 1b: DOS of (0001) beryllium 5-layer slab.

3.2. Potential energy surface

The potential energy surface associated to the tungsten atom approaching the (0001) Be surface (Figure 2a) is presented in Figure 3. Only the W – Be surface and the beryllium atoms of the two deepest layers are frozen at each point of the PES calculation, all the other coordinates are optimized without any constraint; the consequence is that the original symmetry is lost. Coming from 5 Å above the surface, the W atom is trapped without barrier in a deep potential well (***A*** point, ΔE = -4.2 eV). Of course, this scheme implies that the impinging atom is already isolated and detached from the tungsten substrate. This unstable situation is, however, a realistic assumption at the first wall of a fusion device.

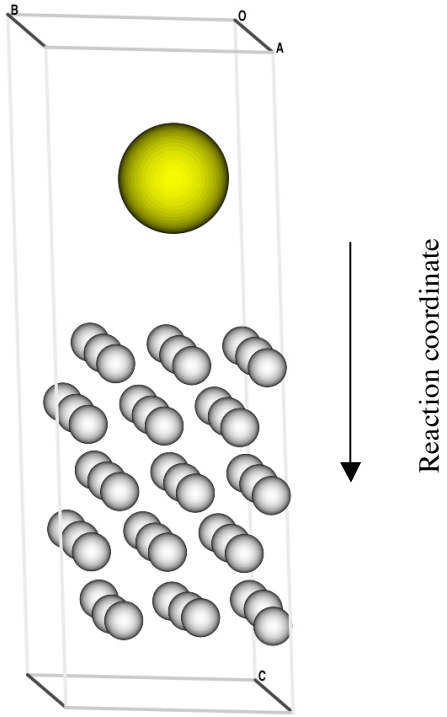

Figure 2a: Crystal working cell of the beryllium metal (0001) film

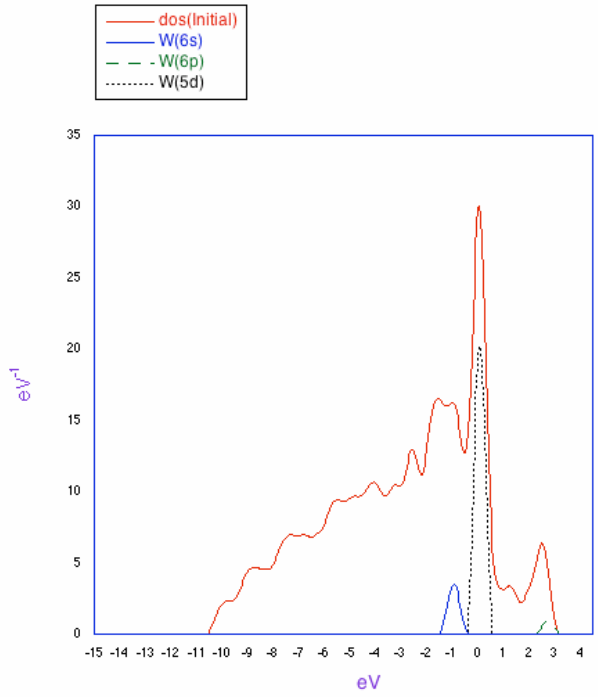

Figure 2b: Total DOS at the initial point (5 Å above the surface)

The beryllium - tungsten reaction is made possible by the tungsten electronic structure. As it can be observed in Figure 2b, the Fermi level of the system slab + W atom falls in the middle of the tungsten *d* band and a contribution of the *s* band of the same element lies right below (-1 eV). When W is adsorbed (***A*** point), the metal surface interaction induces an enlargement of the *d* band through combination with the beryllium orbitals and a net charge transfer from W to Be (~0.5 electron). This is combined with transfer into the W structure from the *s* to the *d* and *p* W levels (Table 1).

Table 1: Löwdin W atom charges (in electrons). ***A*** and ***E*** referred to PES displayed in Figure 3.

	Total charge	*s*	*p*	*d*
W atomic (from pseudopotential)	14.0	4.0	6.0	4.0
W metal	13.99	2.31	6.98	4.70
PES starting point	13.90	4.01	6.02	3.86
A point	13.54	2.38	6.27	4.89
E point	13.63	2.21	6.61	4.81
$Be_{12}W$	13.57	2.19	6.58	4.80

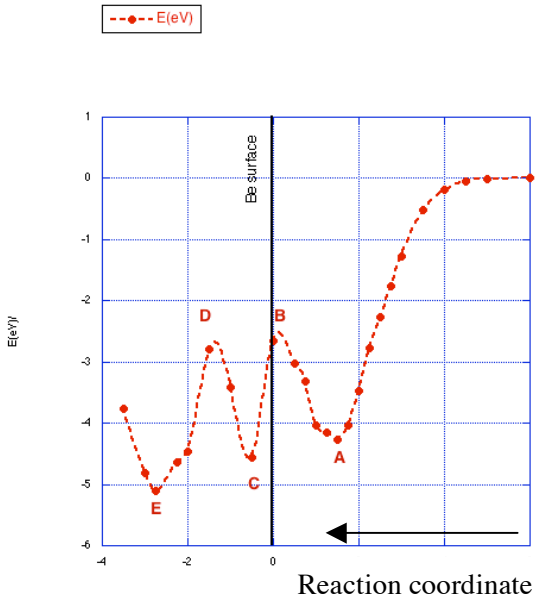

Figure 3a : PES associated to a tungsten atom approaching the surface (structure displayed on Figure 2a), the origin is fixed to the crystal surface.

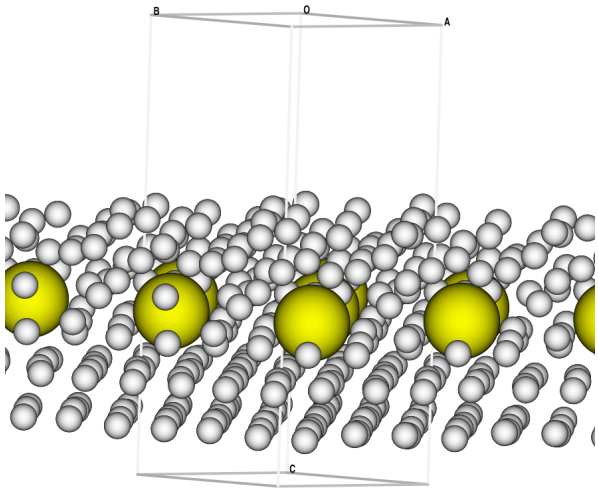

Figure 3b: Structure of the $Be_{44}W$ alloys at the minimum (***E***) of the PES presented on Fig 3a.

Crossing the crystal surface means that an activation barrier of 1.6 eV (***B*** point in Figure 3a) has to be overcome. Beyond this point, the substrate – impurity interaction energy is -4.5 eV (***C*** point), which is comparable to the adsorption energy and of the same order of magnitude as a usual chemical bond. The barrier associated to the second layer is similar to the former one (1.8 eV). The final interaction energy is -4.8 eV in the middle of the working cell (***E*** point). The structure of this *alloy* is displayed on Figure 3b. Due to the very small size of the system and the minimization scheme we had to adopt (freezing of the deepest layers), this result must be considered with precaution. given the small size of this system, this result must be considered with precaution, more especially as neither time nor the temperature intervenes in this calculation. Nevertheless, it can be observed that the beryllium crystal tends to reorganized itself above the W impurity. The first neighbors Be – W bond lengths are ranging from 2.45 to 2.78 Å.

The charge transfer from W to Be is stabilized at a value of about 0.4 electrons. The W *s* type contribution is again confined into the inner shells, as in the tungsten metal. The system stability is ensured by the combination of the *p* and *d* orbitals (Table 1 and Figure 4a). The *d* contribution presents two main peaks below the Fermi level at -1 and -2.2 eV and a peak at 1.6 eV in the conduction band.

Comparison of the above $Be_{44}W$ electronic with experiment is not easy but, according to [19], the Be-W phase diagram presents several stable tungsten-beryllium alloys. $Be_{12}W$ and $Be_{22}W$ are all stable beryllides at low W concentration (less than 10%) and temperature T below 1500°C. $Be_{12}W$ is isostructural with $Mn_{12}Th$ [20] and belongs to the space-group I4/mmm, the GGA-PBE optimized cell parameters are $\boldsymbol{a}$ = 7.260Å, $\boldsymbol{c}$ = 4.112 Å. The calculated cohesive energy is 3.12 eV. This corresponds to two Be - W bond lengths of 2.55 and 2.77 Å, i.e. close to those in $Be_{44}W$.

The W part of the DOS presented in Figure 4a is also very similar to the $Be_{12}W$ one (Figure 4b): the characteristic three *d* peaks are observable but at -2.9, -0.6 and 0.6 eV. In both cases, the *s* and *p* contributions disappear from the region close to the Fermi level and are rejected towards deeper energy zones of the valence band.

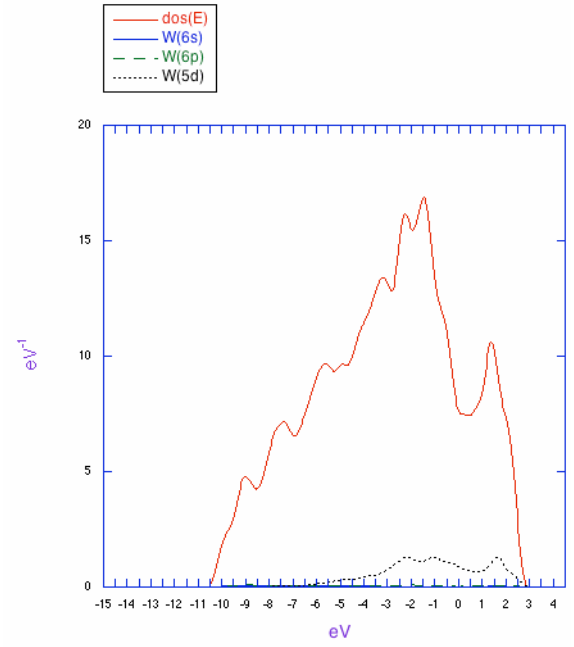

Figure 4a: $Be_{44}W$ DOS at the end of the reaction (***E*** point on the PES).

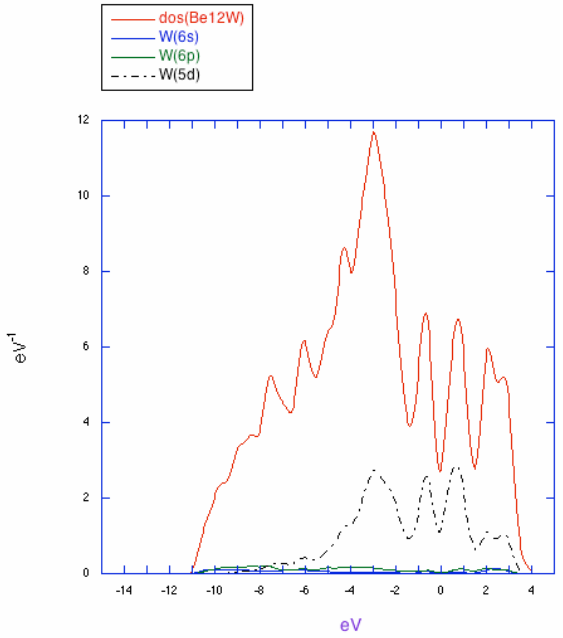

Figure 4b: DOS of the $Be_{12}W$ tungsten beryllide alloy

3.3. Discussion and conclusion

In the paper [4] Linsmeier et al. reported on the formation of beryllium – tungsten mixed materials after thermal diffusion of a tungsten film deposited on a beryllium substrate. In this paper it was pointed out that alloy formation between a tungsten film and a beryllium substrate starts at a temperature of 1070 K, below which there is no indication for alloying or intermixing of Be and W by diffusion. This shows that there is a barrier to the diffusion of the tungsten into beryllium. At 1070 K, the formation of the $Be_{12}W$ alloy can be described by a simple diffusion model without any additional activation barrier. Alloying continues with time until all available W is converted into $Be_{12}W$. This is in good agreement with the DFT results where the activation barriers for the subsurface diffusion (***A*** to ***B*** in the PES) and the diffusion within the bulk (***C*** to ***D*** in the PES) are approximately equal. The $Be_{12}W$ alloy phase formation was identified quantitatively by means of accelerator-based ion beam analysis which confirms the $Be_{12}W$ stoichiometry of the formed alloy. Additionally, X-ray photoelectron spectroscopy (XPS) showed that the Be 1*s* signal of the formed alloy is shifted with respect to the Be metal signal. This indicates changes in the electronic structure associated with the alloy formation. Figure 5 compares the Be 1*s* photoelectron binding energy region of two Be-W alloys (namely $Be_{12}W$ and Be_2W) with the spectrum of a metallic Be film on a tungsten substrate. The

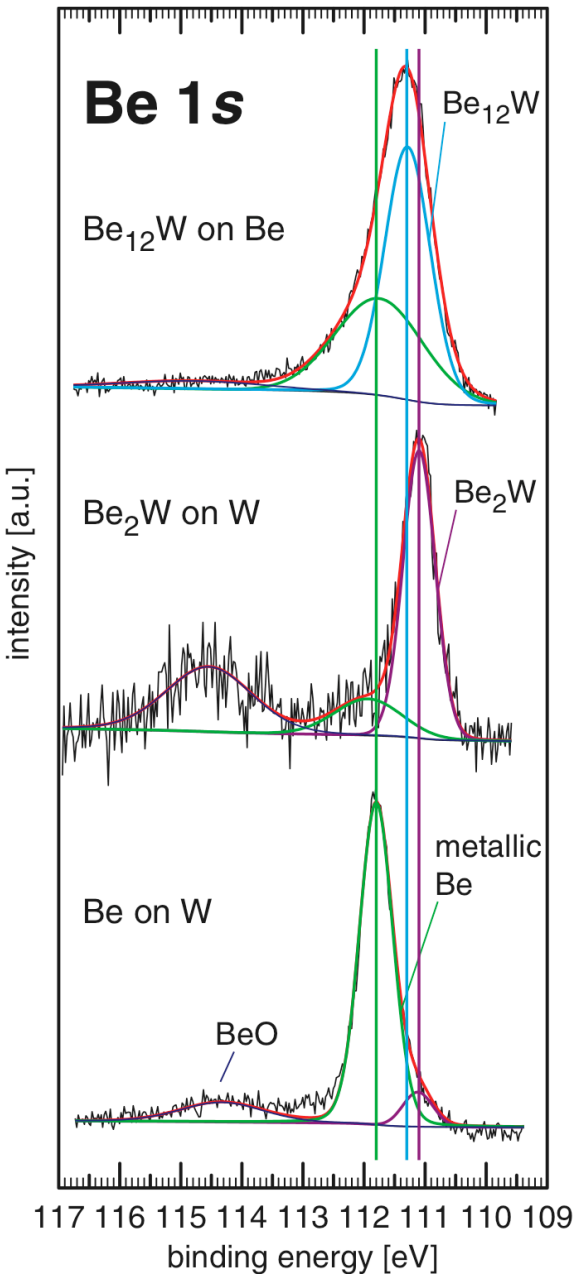

Figure 5: Be 1*s* core level photoelectron spectra measured by XPS, showing the chemical shifts in the Be 1*s* peak in metal and the alloys $Be_{12}W$ and Be_2W.

photoelectron spectra are fitted with Gauss-Lorentz functions, representing the metallic signal, an alloy peak and a peak associated with Be in BeO. The metallic Be film and the Be_2W film on W were prepared and measured in an in situ experiment [21] where Be has been evaporated on W substrates at room temperature. After deposition, directly at the interface the formation of a Be_2W interface layer was observed. During annealing, additional Be_2W surface alloy has been formed. The 2:1 stoichiometry of the Be_2W surface alloy has been confirmed by XPS after 970 K annealing. The chemical shift of Be 1*s* in the Be_2W alloy is determined to -0.7 eV compared to the Be metal signal at 111.8 eV.

In case of the $Be_{12}W$ alloy, a peak shift of the Be 1*s* signal of -0.4 eV with respect to the metallic signal has been identified. This is shown in the upper spectrum of Figure 5. This spectrum is measured after sputtering of the alloy film by Ar ions, since the sample has been transported through air between the annealing and measurement steps. Therefore, the peak shift attributed to the Be_2W alloy is experimentally more reliable than the shift attributed to the $Be_{12}W$ stoichiometry. Nevertheless, the Be 1s shifts in both identified Be-W alloys demonstrate changes in the electronic structures upon alloy formation, compared to metallic Be. Similar shifts are also observed in the W 4*f* peaks and also visible in the valence band spectral regions, as demonstrated for Be_2W in [21].

The quantum calculation indicates that even if the tungsten adsorption is a barrier-free process, a W atom reaching the Be surface with a low impact energy will be strongly adsorbed, therefore a pure tungsten film could build up on the beryllium film thus interfering with the diffusion of the subsequent impinging W.

If this barrier is overcome, or if the kinetic energy of the tungsten atom is large enough, the barrier to diffusion into the bulk and alloy formation is relatively low and the process can further develop until a new adsorbed protective film is again formed.

Unfortunately the calculation of the Be 1*s* level shift is not an easy task, but the comparison we made between the beryllide DOS around the Fermi level and the $Be_{12}W$ DOS, together with the confrontation of the Be – W bond length all highlight the similarities of the two structures. The next step of the study would be to include the temperature and kinetic energy parameters into the theoretical simulation; this will be the matter of our next paper [22].

Acknowledgments

This work is partially supported by the Euratom–CEA Association, in the framework of the *Fédération de Recherche Fusion par Confinement Magnétique,* and by the Agence Nationale de la Recherche (ANR CAMITER n° ANR-06-BLAN-0008-01). The calculations were performed at the CEA *(CCRT*) and CNRS (*IDRIS*) computing Centers.

References

[1] Wesson J 2004 *Tokamaks* (Oxford: Oxford Science Publications)
[2] http://www.iter.org/
[3] Doerner R P 2007 *J. Nucl. Mater.* **363-365** 32
[4] Linsmeier Ch, Ertl K, Roth J, Wiltner A, Schmid K, Kost F, Bhattacharyya S R, Baldwin M and Doerner R P 2007 *J. Nucl. Mater.* **363-365** 1129
[5] Scandolo S, Giannozzi P, Cavazzoni C, de Gironcoli S, Pasquarello A and Baroni S 2005 *Z. Kristallogr.* **220** 574; Quantum Espresso website *http://www.quantum-espresso.org*
[6] Allouche A to be published
[7] Martin J M L 1999 *Chem.Phys.Lett* **303** 399
[8] Røeggen I and Veseth L 2005 *Int.J.Quant.Chem.* **101** 201
[9] Wang J, Wang G and Zhao J *J. Phys.: Condens. Matter.* 2001 **13** L753
[10] Cerowski V, Rao B K, Khanna S N, Jena P, Ishii S, Ohno K and Kawazoe Y 2005 *J.Chem.Phys.* **123** 74329
[11] Dovesi R, Pisani C, Ricca F and Roetti C 1982 *Phys. Rev.* **25** 3731
[12] http://www.crystal.unito.it
[13] Wachowicz E and Kiejna A 2001 *J.Phys.: Condens. Matter.* **13** 10767
[14] Lazzeri M and de Gironcoli S 2000 *Surf. Sci.* **454-456** 442
[15] Holtzwarth N A W and Zeng Y 1995 *Phys. Rev. B* **51** 13653
[16] Häussermann U and Simak S I 2001 *Phys. Rev.* **64** 245114
[17] Angonoa G, Koutecky J and Pisani C 1982 *Surf. Sci.* **121** 355
[18] Lazzeri M and de Gironcoli S 1998 *Surf. Sci.* **402-404** 715
[19] Okammoto H, Tanner L E 1991 *Phase Diagrams of Binary Tungsten Alloys* (Calcutta: Indian Institute of Physics) ed. S V Nagendra Naidu and P Ramo Rao
[20] Batchelder F W and Raeuchle R F 1957 *Acta Cryst.* **10** 648
[21] Wiltner A and Linsmeier Ch 2006 *New J. Phys.* **8** 181
[22] Allouche A *in preparation*